

PHASE EQUILIBRIA IN THE CuSbS₂ - Sb₂S₃ - SbSI COMPOSITION RANGE OF THE Cu-Sb-S-I QUATERNARY SYSTEM

Dunya M. Babanly^{1,2*}, Darvin R. Mammadli^{1,2}, Ganira B. Dashdiyeva³, Dilgam B. Tagiyev²

Abstract. The phase equilibria in the $CuSbS_2$ - Sb_2S_3 - SbSI compositions intervals of the Cu-Sb-S-I quaternary system have been investigated by differential thermal analysis and X-ray phase analysis methods. The boundary quasi-binary section $CuSbS_2$ - SbSI, two internal polythermal sections of the phase diagram, as well as, the projection of the liquidus surface of the system were constructed. Primary crystallization areas of phases, types and coordinates of non- and monovariant equilibria were determined. It was established that, the system is quaternary and belongs to the nonvariant eutectic type. The liquidus surface consists of three distinct regions, each representing the direct crystallization of one of the primary compounds from the melt. These regions are separated by three eutectic curves defining the boundaries between them.

Keywords: DTA, XRD, phase diagram, chalcostibite, stibnite, antimony sulfoiodide.

Corresponding Author: Dunya Mahammad Babanli, French - Azerbaijani University (UFAZ), Azerbaijan State Oil and Industry University (ASOIU), Baku, Azerbaijan; Institute of Catalysis and Inorganic Chemistry (ICIC), Baku, Azerbaijan, e-mail: dunya.babanly@ufaz.az

Received: 6 January 2025; Accepted: 26 February 2025; Published: 9 April 2025.

1. Introduction

The study of phase equilibria in multicomponent systems is essential for understanding the thermodynamic stability and phase relationships of materials with potential technological applications. These studies are particularly important for systems involving sulfides, which are of significant interest due to their applications in emerging technologies such as photovoltaics, thermoelectric devices, optoelectronics and environmental sensors etc. (Ivanov-Shic & Murin, 2000; Babanly *et al.*, 2019; Jamal *et al.*, 2023; Saeed *et al.*, 2024; Babanly *et al.*, 2024; Mashadiyeva *et al.*, 2024; Aliyev *et al.*, 2024). The system CuSbS₂ - Sb₂S₃ - SbSI (A) represents a chemically rich region of interest due to the unique properties of its constituent compounds, which are widely recognized for their applications in advanced technologies.

How to cite (APA):

Babanly, D.M., Mammadli, P.R., Dashdiyeva, G.B., Ahmadov, E.J. & Tagiyev, D.B. (2025). Phase equilibria in the CuSbS₂ - Sb₂S₃ - SbSI composition range of the Cu-Sb-S-I quaternary system. *New Materials, Compounds and Applications*, 9(1), 40-49 https://doi.org/10.62476/nmca.9140

¹French - Azerbaijani University (UFAZ), Azerbaijan State Oil and Industry University (ASOIU), Baku, Azerbaijan

²Institute of Catalysis and Inorganic Chemistry (ICIC), Baku, Azerbaijan

³Baku Engineering University (BEU), Baku, Azerbaijan

⁴Azerbaijan State University of Economics (UNEC), Baku, Azerbaijan

Most ternary Cu-Sb-sulfides are naturally occurring minerals that have been extensively studied for their potential as electronic materials, exhibiting remarkable properties such as high photoelectric performance, photovoltaic efficiency, radiation detection capabilities and thermoselectric functionality. Their abundance in nature and environmentally friendly characteristics have further driven recent research advancements in these materials (Chetty et al., 2015; Loranca-Ramos et al., 2017; Van Embden et al., 2013; Lu et al., 2012). CuSbS₂ (chalcostibite) is a p-type semiconductor known for its potential in solar energy applications due to its direct bandgap and earthabundant, non-toxic constituents (Yang et al., 2014; Van Embden et al., 2020; Wang et al., 2021; Welch et al., 2016; Mashadiyeva et al., 2021). Sb₂S₃ (stibnite), an antimony sulfide mineral, has garnered attention for its high optical absorption coefficient and excellent thermoelectric properties (Mashadiyeva et al., 2021; Farhana & Bandara, 2022; Ishaq et al., 2020; Kondrotas et al., 2018; Zhang et al., 2018). Similarly, SbSI exhibits remarkable pyroelectric and piezoelectric properties, making it suitable for optical and energy conversion applications (Simsek et al., 2015; Tamilselvan & Bhattacharyya, 2016; Brown et al., 1996; Surthi et al., 2002).

Understanding the phase relationships within this ternary system is critical for tailoring materials with optimized properties for specific applications. Furthermore, the coexistence of these phases at varying compositions and temperatures offers insights into the stability of complex sulfide-based systems. This study, as a continuation of our systematic studies in the Cu-Sb-S-I quaternary system (Mammadli $et\ al.$, 2022a, 2022b, 2021, 2023), focuses on the systematic investigation of the phase equilibria in CuSbS2 - Sb2S3 - SbSI composition range. The research aims to construct a comprehensive phase diagram, identify the stable and metastable phases, understand the interactions and compatibility of the components and explore how thermal and compositional variations influence the system's behavior. The results of this work will not only advance the fundamental understanding of complex sulfide systems but also provide a valuable framework for the development of novel materials with applications in energy, electronics and environmental technologies.

Two boundary sections of the CuSbS₂-Sb₂S₃-SbSI subsystem, specifically the CuSbS₂-Sb₂S₃ and Sb₂S₃-SbSI systems, have been studied in earlier research. Both systems form a simple eutectic phase diagram (Babanly *et al.*, 1993; Aliyev *et al.*, 2017).

The phase relationships within the $CuSbS_2$ -SbSI boundary system have been investigated for the first time in this study and the findings will be thoroughly examined and discussed in the subsequent sections of this paper.

2. Experimental part

Alloys of the system were prepared from the preliminarily synthesized and identified Sb₂S₃, CuSbS₂ and SbSI compounds. Elemental copper, antimony, sulphur and iodine of high purity from Alpha Aesar and Sigma Aldrich were used for synthesis.

Initial binary (Sb₂S₃) and ternary (CuSbS₂ and SbSI) compounds were synthesized from the elemental components in an evacuated (~10⁻² Pa) silica ampoules followed by a specially designed method taking into account the high volatility of iodine and sulfur. The synthesis was performed in an inclined two-zone furnace, with the hot zone kept at a temperature 20-30⁰C higher than the corresponding melting point of the synthesized compound, whereas the temperature of the cold zone was kept at about 400K considering the high vapor pressure of iodine. After the main portion of iodine and sulfur had reacted,

the ampoules were relocated such that the products could melt at relevant melting temperatures. Ampoules were kept stirring at corresponding temperatures for 2 hours and the furnaces cooled gradually. The purity and individuality of the obtained products were monitored using differential thermal analysis (DTA) and powder X-ray diffraction (PXRD) methods. The heating curves and the diffraction pattern for some of the constituent compounds of the system under study are given in Figure 1 and 2. Both methods prove identity and purity of the synthesized compounds.

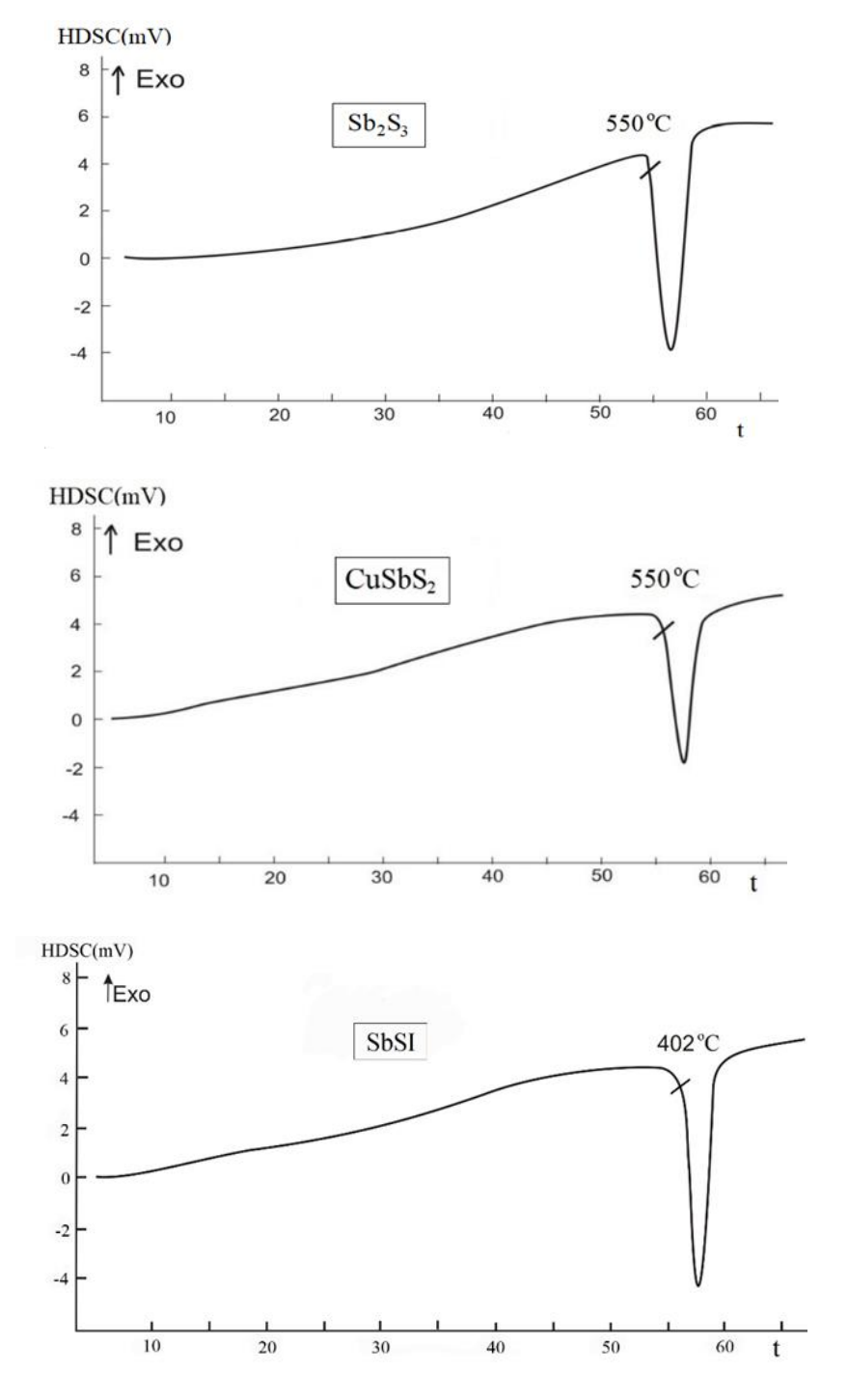


Figure 1. Heating curves of the constituent compounds of the system CuSbS₂ – Sb₂S₃ – SbSI

Two sets of samples (0.5 g by mass each) were prepared by co-melting of different proportions of the preliminarily synthesized binary and ternary compounds. After melting, most of the alloys were annealed at about ~20-30°C below the solidus temperature for ~800 hours in order to achieve complete homogenization.

The DTA and PXRD techniques were employed to verify the purity and identity of the synthesized compounds, as well as to perform experimental investigations. DTA of the samples was conducted in evacuated quartz ampoules using a 404 F1 Pegasus System differential scanning calorimeter. The measurement data were analyzed with the NETZSCH Proteus Software, ensuring a temperature accuracy of $\pm 2^{0}$ C. XRD analysis of the annealed alloys was performed at room temperature using a Bruker D2 PHASER diffractometer with CuK α_{1} radiation. The diffraction patterns were indexed using the Topas 4.2 Software.

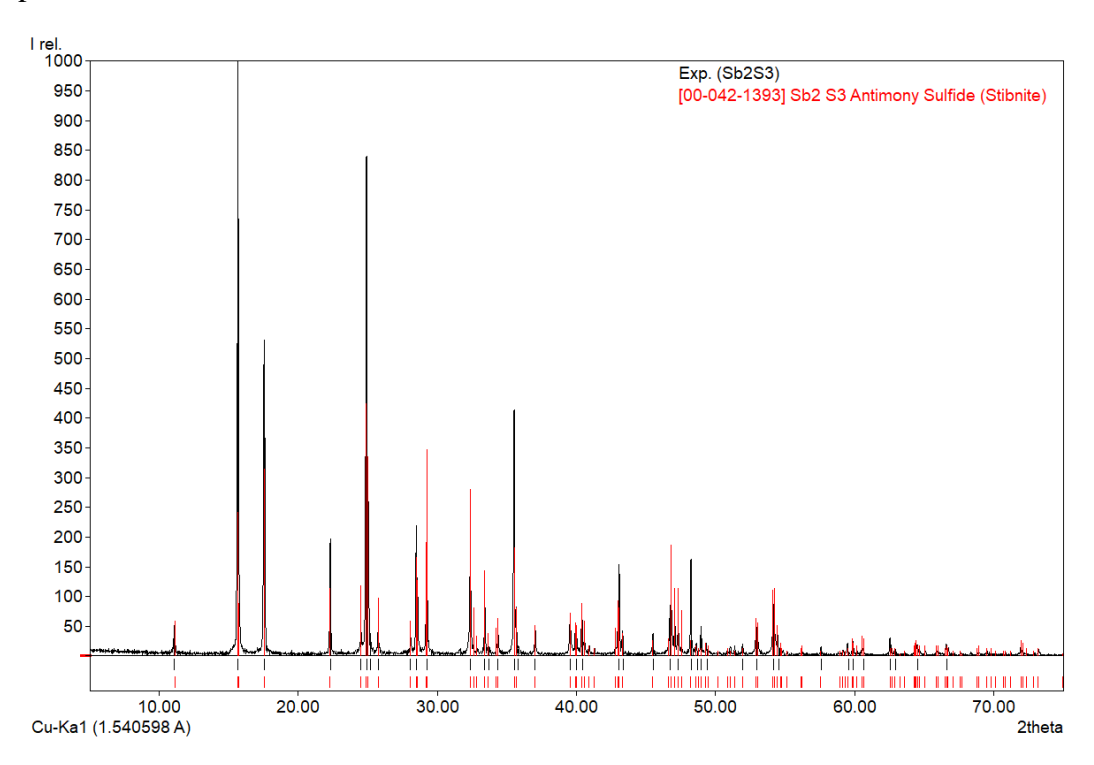


Figure 2. Diffraction pattern of the Sb₂S₃ compound

3. Results and discussion

On the phase diagram of the system $CuSbS_2 - Sb_2S_3 - SbSI$ and its various sections, the compositions of alloys are expressed in equal numbers of atoms using the corresponding coefficients in front of their formulas. This is identical to the expression of composition in atomic percent and allows these data to be used in the general phase diagram of the Cu-Sb-S system without recalculation of composition.

3.1. CuSbS₂ - SbSI boundary quasi-binary system

The phase diagram of the $CuSbS_2$ - SbSI boundary system is quasi binary due to the congruent melting character of its both compounds. As it can be seen from the T-x diagram constructed based on the DTA results (Figure 3), the system is of a simple eutectic type. Eutectic equilibrium

$$L \leftrightarrow CuSbS_2 + SbSI \tag{1}$$

is established at 385 °C and ~72 mol% SbSI composition.

By constructing the Tamman triangle, it was determined that solubility based on the initial compounds is practically nonexistent and the composition of the eutectic was clarified (Figure 3).

The constructed phase diagram was also confirmed using the powder PXRD method. Figure 4 presents the powder diffraction patterns of samples with various compositions along the system. As observed, the diffraction patterns of all intermediate alloys are two-phase, consisting of the combined reflection lines of the initial compounds that constitute the system.

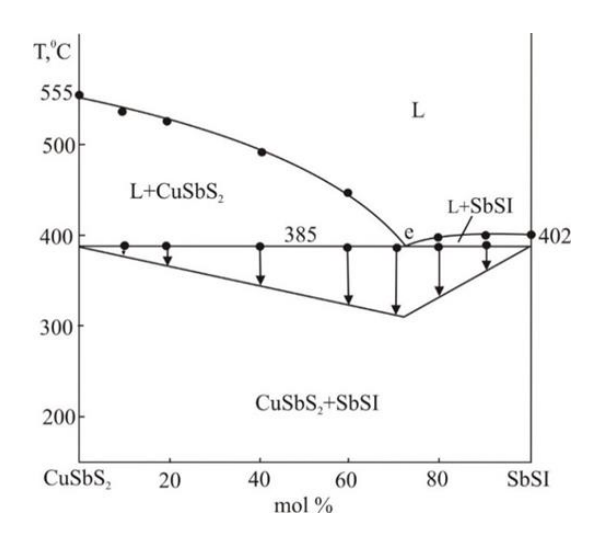


Figure 3. T-x phase diagram of the system CuSbS₂ - SbSI

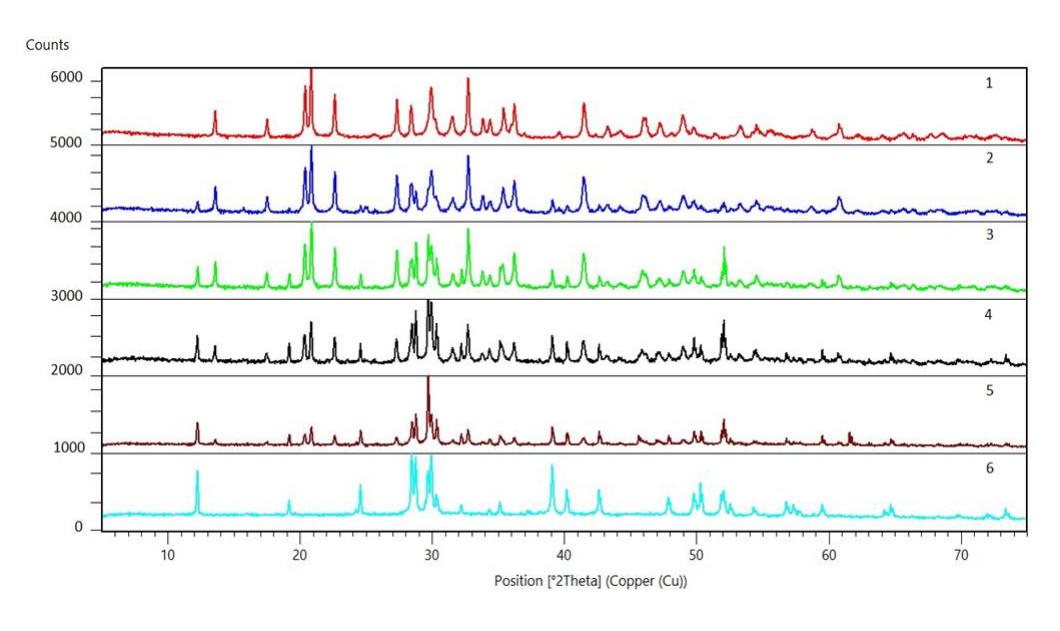


Figure 4. PXRD spectrums of some alloys along the system CuSbS₂ – SbSI. Composition of alloys: 1 - SbSI; 2 - 80 mol % SbSI; 3 - 60 mol % SbSI; 4 - 40 mol % SbSI; 5 - 20 mol % SbSI; 6 - CuSbS₂

3.2. Projection of the liquidus surface (Figure 5)

The projection of the liquidus surface of the system A on the concentration triangle is given in Figure 5. As previously noted, all three boundary sections of the system are quasi-binary, which means that the concentration triangle CuSbS₂-Sb₂S₃-SbSI represents an independent subsystem. The liquidus surface of the system (A) is characterized by non-variant eutectic equilibrim.

The liquidus surface consists of three regions that represent the direct crystallization of the primary compounds from the melt. These regions are bounded by three eutectic curves that connect them.

The eutectic points of the side quasibinary systems are characterized by the following coordinates:

e₁: 496 ⁰C and 60 mol% Sb₂S₃,

e₂: 385 ⁰C and 72 mol% SbSI,

e₃: 387 ⁰C and 70 mol% SbSI.

The curves originating from these points, denoted as e_1E , e_2E and e_3E , represent the monovariant eutectic equilibria:

$$Le_1E \leftrightarrow CuSbS_2 + Sb_2S_3 (496 - 365^0C)$$
 (2)

$$Le_2E \leftrightarrow CuSbS_2 + SbSI (385 - 365^{\circ}C)$$
 (3)

$$Le_3E \leftrightarrow Sb_2S_3 + SbSI (387-365^0C) \tag{4}$$

The ternary eutectic point (E) is characterized by a temperature of $365\,^{\circ}\text{C}$ and reflects the nonvariant eutectic crystallization of the primary compounds from the liquid phase:

$$L_E \leftrightarrow CuSbS_2 + Sb_2S_3 + SbSI \tag{5}$$

All samples within the system, regardless of composition, undergo complete crystallization following this reaction (Figure 5).

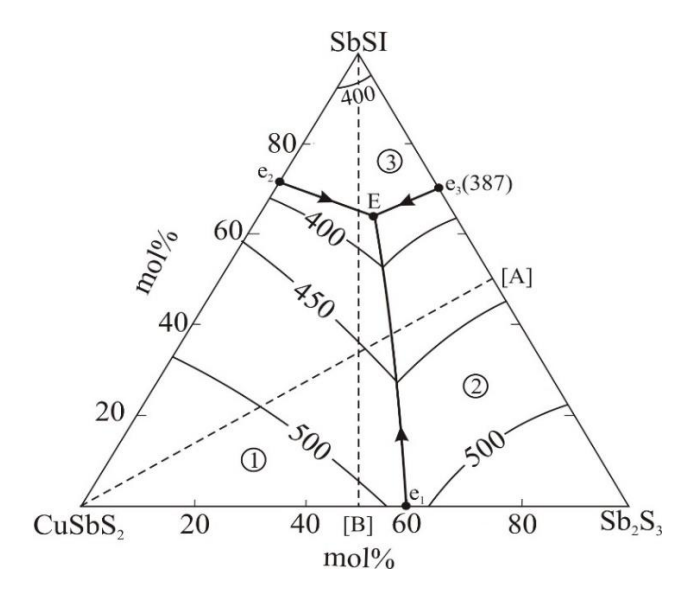


Figure 5. Projection of the liquidus surface of the system CuSbS₂-Sb₂S₃-SbSI. Primary crystallization fields: 1 - CuSbS, 2 - Sb₂S₃; 3 - SbSI. Dotted lines are studied polythermal sections

3.3. Polythermal sections

The CuSbS₂ - [A] (Figure 6) and SbSI - [B] (Figure 7) polythermal sections of the system A are given below and analyzed in context with the projection of the liquidus surface (Figure 5) of the system. Here, [A] and [B] are 1:1 mix ratios of the constituent compounds of the relevant side binary systems, consequently.

The system $CuSbS_2$ - [A] (Figure 6).

This section passes through the liquidus surfaces of the $CuSbS_2$ and Sb_2S_3 compounds and intersects the eutectic equilibrium curve e_1E . The left branch of the liquidus reflects the primary crystallization of the $CuSbS_2$ compound from the molten alloy, while the right branch corresponds to the primary crystallization of the Sb_2S_3 compound. The intersection point of these curves (~26 mol% $CuSbS_2$, 430 °C) marks the onset of the crystallization of the $CuSbS_2 + Sb_2S_3$ eutectic mixture according to the monovariant reaction (2).

Below the liquidus curves, crystallization proceeds via the reactions described by (3) and (4). This leads to the formation of two three-phase regions in the phase diagram: $L + CuSbS_2 + Sb_2S_3$ and $L + Sb_2S_3 + SbSI$. The crystallization process concludes with the nonvariant eutectic reaction (5), represented by a horizontal line at 365°C.

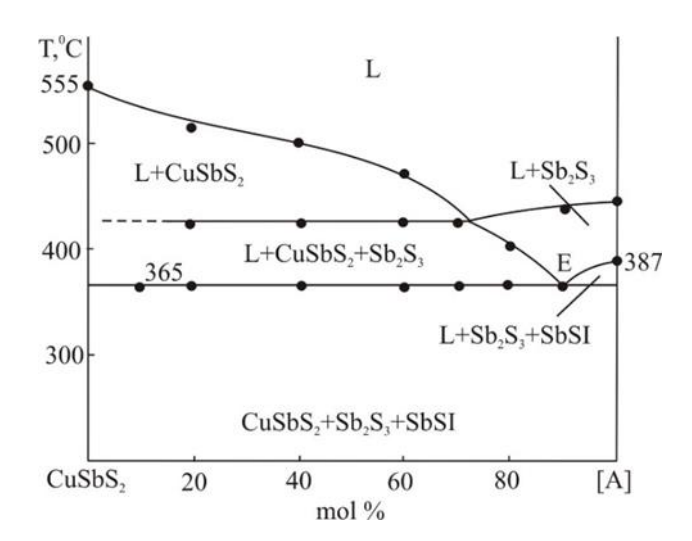


Figure 6. T-x phase diagram of the $CuSbS_2$ - [A] polythermal section

The system Sb_2S_3 - [B] (Figure 7)

This section passes through the primary crystallization surfaces of the $CuSbS_2$ and SbSI compounds and intersects the eutectic curve e_2E . In the composition range of 0-65 mol% SbSI, $CuSbS_2$ crystals are the first to precipitate from the liquid phase, while in the range of 65-100 mol% SbSI, the crystals of SbSI are the primary phases to crystallize. Below the liquidus, crystallization proceeds through the monovariant eutectic reactions described by (2) and (3), leading to the formation of two three-phase regions on the T-x diagram: $L + Sb_2S_3 + CuSbS_2$ and $L + Sb_2S_3 + SbSI$. Finally, the complete crystallization of all samples occurs at 365 °C through the nonvariant eutectic reaction described by (5).

In Figure 7, a portion of the liquidus curve for the $CuSbS_2$ compound and the horizontal line corresponding to reaction (3) are shown as dashed lines. This representation is due to the low intensity of the effects associated with these processes on the DTA curves and their overlap with more intense nearby peaks.

In conclusion, it should be noted that the DTA results of several additional samples along the two examined polythermal sections have allowed for a more precise determination of the trajectories of isotherms on the liquidus surfaces, the paths of monovariant equilibrium curves and the coordinates of the ternary eutectic point.

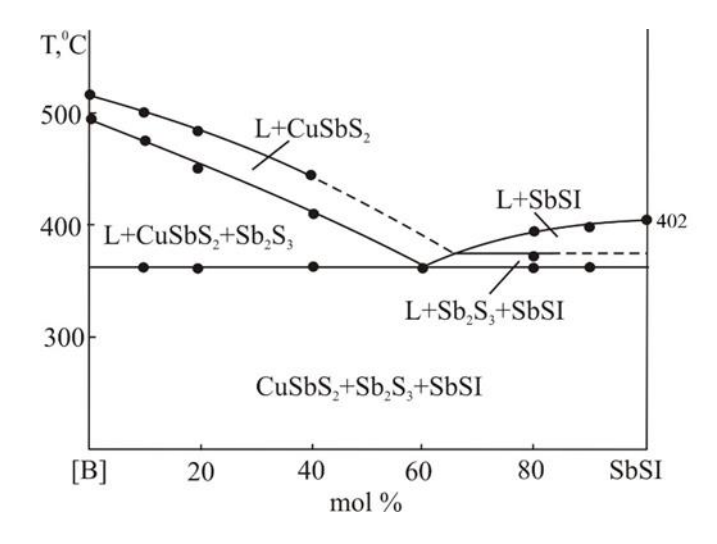


Figure 7. T-x phase diagram of the [B] - SbSI polythermal section

4. Conclusion

The phase equilibria in the CuSbS₂ - Sb₂S₃ - SbSI composition range of the Cu-Sb-S-I quaternary system have been studied for the first time. Several polythermal sections of the phase diagram including the CuSbS₂-SbSI boundary system and T-x-y projection of the liquidus surface of the system were obtained by co-analysis of experimental results along with the literature data on boundary binary systems. It was defined that the system is of eutectic type. Types and coordinates of non- and monovariant equilibria, as well as, primary crystallization areas of phases were determined.

References

Aliev, Z.S., Musayeva, S.S. & Babanly, M.B. (2017). The phase relationships in the Sb-S-I system and thermodynamic properties of the SbSI. *Journal of Phase Equilibria and Diffusion*, 38(6), 887-896. https://doi.org/10.1007/s11669-017-0601-4

Aliyev, F.R., Orujlu, E.N., Mashadiyeva, L.F., Dashdiyeva, G.B. & Babanly, D.M. (2024). Solid - phase equilibria and thermodynamic properties of the Sb-Te-S system. *Physics and Chemistry of Solid State*, 25(1), 26-34. https://doi.org/10.15330/pcss.25.1.26-34

Babanly, M.B., Mashadiyeva, L.F., Babanly, D.M., Imamaliyeva, S.Z., Tagiev, D.B. & Yusibov, Yu.A. (2019). Some issues of complex studies of phase equilibria and thermodynamic properties in ternary chalcogenide systems involving EMF measurements (review). *Russian Journal of Inorganic Chemistry*, 64(13), 1649-1671. https://doi.org/10.1134/s0036023619130035

Babanly, M.B., Yusibov, Y.A., Imamaliyeva, S.Z. Babanly, D.M. & Alverdiyev, I.J. (2024). Phase diagrams in the development of the argyrodite family compounds and solid solutions based on them. *Journal of Phase Equilibria and Diffusion*, 45, 228-255. https://doi.org/10.1007/s11669-024-01088-w

Babanly, M.B., Yusibov, Yu.A. & Abishev, V.T. (1993). *Three-Component Chalcogenides Based on Copper and Silver*. Baku: BSU, 342. (In Russian).

- Brown, M.P., Newnham, S.J. & Smith, P.W. (1996). The application of SbSI and other ferroelectric materials to the generation of solitons and shock waves on nonlinear high voltage transmission lines. *Seventh International Conference on Dielectric Materials, Measurements and Applications*, 76-81. https://doi:10.1049/cp:19960995
- Chetty, R., Bali, A. & Mallik, R.C. (2015). Tetrahedrites as thermoelectric materials: An overview. *Journal of Materials Chemistry C*, 3(48), 12364-12378. https://doi.org/10.1039/c5tc02537k
- Farhana, M.A., Bandara, J. (2022). Enhancement of the photoconversion efficiency of Sb₂S₃ based solar cell by overall optimization of electron transport, light harvesting and hole transport layers. *Solar Energy*, 247, 32-40. https://doi.org/10.1016/j.solener.2022.10.025
- Ishaq, M., Chen, S., Farooq, U., Azam, M., Deng, H., Su, Z.H., ... & Liang, G.X. (2020). High open-circuit voltage in full-inorganic Sb₂S₃ solar cell via modified Zn-doped TiO₂ electron transport layer. *Solar RRL*, 4(12), 2000551. https://doi.org/10.1002/solr.202000551
- Ivanov-Shic, A.K., Murin, I.V. (2000). Solid Ionics. St. Petersburg: Publishing house of St. Petersburg State University, 616. (In Russian).
- Jamal, F., Rafique, A., Moeen, S., Haider, J., Nabgan, W., Haider, A., ... & Maqbool, M. (2023). Review of metal sulfide nanostructures and their applications. *ACS Applied Nano Materials*, 6(9), 7077-7106. https://doi.org/10.1021/acsanm.3c00417
- Kondrotas, R., Chen, C. & Tang, J. (2018). Sb₂S₃ solar cells. *Joule*, 2(5), 857-878.
- Loranca-Ramos, F., Diliegros-Godines, C., González, R.S. & Pal, M. (2017). Structural, optical and electrical properties of copper antimony sulfide thin films grown by a citrate-assisted single chemical bath deposition. *Applied Surface Science*, 427, 1099-1106. https://doi.org/10.1016/j.apsusc.2017.08.027
- Lu, X., Morelli, D.T., Xia, Y., Zhou, F., Ozolins, V., Chi, H., ... & Uher, C. (2012). High performance thermoelectricity in Earth-Abundant compounds based on natural mineral tetrahedrites. *Advanced Energy Materials*, *3*(3), 342-348. https://doi.org/10.1002/aenm.201200650
- Mammadli, P.R., Babanly, D.M. (2023). Powder x-ray diffraction study of the Cu₃SbS₃ CuI system. *Chemical Problems*, *1*(21), 57-63. https://doi.org/10.32737/2221-8688-2023-1-57-63
- Mammadli, P.R., Gasimov, V.A. & Babanly, D.M. (2022). Phase relations in the Cu₃SbS₄-Sb₂S₃ S system. *Chemical Problems*, 1(20), 40-48. https://doi.org/10.32737/2221-8688-2022-1-40-47
- Mammadli, P.R., Gasimov, V.A., Mashadiyeva, L.F. & Babanly D.M. (2022). Phase relations in the CuSbS₂ Sb₂S₃ Sb system. *New Materials, Compounds and Applications*, 6(1), 37-43.
- Mammadli, P.R., Mashadiyeva, L.F., Gasimov, V.A., Dashdiyeva, G.B. & Babanly, D.M. (2021). Phase relations in the CuSbS₂-Cu₃SbS₄- Sb₂S₃ system. *AJCN*, 3(1), 100-108.
- Mashadiyeva, L.F., Babanly, D.M., Hasanova, Z.T., Yusibov Y.A. & Babanly, M.B. (2024). Phase relations in the Cu-As-S System and thermodynamic properties of copper-arsenic sulfides. *Journal of Phase Equilibria and Diffusion*, 45, 567-582. https://doi.org/10.1007/s11669-024-01115-w
- Mashadiyeva, L.F., Mammadli, P.R., Babanly, D.M., Ashirov, G.M., Shevelkov A.V. & Yusibov Y.A. (2021). Solid-phase equilibria in the Cu-Sb-S system and thermodynamic properties of copper-antimony sulfides. *JOM*, 73(5), 1522-1530. https://doi.org/10.1007/s11837-021-04624-v
- Saeed, M., Shahzad, U., Rabbee, M.F., Al-Humaidi, J.Y., Marwani, H.M., Rehman, Sh.Ur., ... & Rahman, M.M. (2024). Comprehensive reviews on the potential applications of inorganic metal sulfide nanostructures in biological, environmental, healthcare and energy generation and storage. *Reviews in Inorganic Chemistry*. https://doi.org/10.1515/revic-2024-0016
- Sımsek, S., Koc, H., Palaz, S., Oltulu, O., Mamedov, A.M. & Ozbay, E. (2015). SbSI based photonic crystal superlattices: Band structure and optics. *IOP Conference Series: Materials Science and Engineering*, 77(1), 012020. https://doi:10.1088/1757-899X/77/1/012020

- Surthi, S., Kotru, S. & Pandey, R.K. (2002). SbSI films for ferroelectric memory applications. *Integrated Ferroelectrics*, 48(1), 263-269. https://doi:10.1080/10584580215458
- Tamilselvan, M., Bhattacharyya, A.J. (2016). Antimony sulphoiodide (SbSI), a narrow band-gap non-oxide ternary semiconductor with efficient photocatalytic activity. *RSC Advances*, 6(107), 105980-105987. https://doi.org/10.1039/C6RA23750A
- Van Embden, J., Latham, K., Duffy, N.W. & Tachibana, Y. (2013). Near-infrared absorbing Cu₁₂Sb₄S₁₃ and Cu₃SbS₄ nanocrystals: Synthesis, characterization and photoelectrochemistry. *Journal of the American Chemical Society*, 135(31), 11562-11571. https://doi.org/10.1021/ja402702x
- Van Embden, J., Mendes, J.O., Jasieniak, J. J., Chesman, A.S.R. & Della Gaspera, E. (2020). Solution-processed CuSbS₂ thin films and superstrate solar cells with CdS/In₂S₃ buffer layers. *ACS Applied Energy Materials*, *3*(8), 7885-7895. https://doi.org/10.1021/acsaem.0c01296
- Wang, L., Zhao, X., Yang, Z., Ng, B.K., Jiang, L., Lai, Y. & Jia, M. (2021). CuSbS₂ solar cells using CdS, In₂S₃ and the In/Cd-based hybrid buffers. *Journal of Electronic Materials*, 50(6), 3283-3287. https://doi.org/10.1007/s11664-021-08815-w
- Welch, A.W., Baranowski, L.L., Zawadzki, P., DeHart, C., Johnston, S., Lany, S., ... & Zakutayev, A. (2016). Accelerated development of CuSbS₂ thin film photovoltaic device prototypes. *Progress in Photovoltaics Research and Applications*, 24(7), 929-939. https://doi.org/10.1002/pip.273
- Yang, B., Wang, L., Han, J., Zhou, Y., Song, H., Chen, S., ... & Tang, J. (2014). CuSbS₂ as a promising earth-abundant photovoltaic absorber material: A combined theoretical and experimental study. *Chemistry of Materials*, 26(10), 3135-3143. https://doi:10.1021/cm500516v
- Zhang, L., Wu, C., Liu, W., Yang, S., Wang, M., Chen, T. & Zhu, C. (2018). Sequential deposition route to efficient Sb₂S2₃ solar cells. *Journal of Materials Chemistry A*, 6(43), 21320-21326. https://doi.org/10.1039/C8TA08296K